



A comprehensive study of high-performance of flexible transparent conductive silver nanowire films

Y. H. Wang¹ · X. Yang^{1,2} · D. X. Du^{1,2} · X. F. Zhang¹

Received: 29 April 2019 / Accepted: 10 June 2019 / Published online: 15 June 2019
© Springer Science+Business Media, LLC, part of Springer Nature 2019

Abstract

In this paper, we systematically investigated the effects of concentration and amount of silver nanowires (AgNWs) suspension on the optoelectronic properties and microstructures of flexible transparent conductive films (FTCFs) composed of AgNWs with an average diameter of about 25 nm and length of 15.5 μm . AgNW–FTCFs were prepared on polyethylene terephthalate substrates using a Meyer rod and then dried in the ambient environment. The experimental results reveal that with increasing of the concentration and amount of AgNWs the sheet resistance and non-uniformity factor (*NUF*) of the sheet resistance and the transmittance of AgNW–FTCFs decreased. while, the root mean square roughness (*RMS*) and the haze value of the AgNW–FTCFs increased. The AgNWs suspension with low concentration and high amount is beneficial to obtain the high-performance conductive film prepared using Meyer rod. The fabricated film exhibit a sheet resistance of 502–38 Ωsq^{-1} and a *NUF* of the sheet resistance of 0.7–0.2% and a haze of 0.77–1.0% at a transmittance of 90–95% and *RMS* value of 11.0–13.1 nm. These *RMS* values are low approximately the diameter of a nanowire. These results are attributed to the good morphology of and uniform distribution of AgNWs.

1 Introduction

Owing to the booming development of flexible and wearable devices, there is enormous demand for the flexible transparent conductive films (FTCFs). The inorganic semiconductor, indium tin oxide (ITO), is the most widely used material due to its high transparency in thin film. However, its brittle ceramic property and expensive vacuum deposition process are limitations to its further progress. Promising candidates for replacing ITO for FTCF applications include metal nanowires [1], single-walled carbon nanotubes (CNT) [2, 3], and graphenes [4], etc.

Silver nanowires (AgNWs) are especially promising due to the higher conductivity when compared to the carbon based CNTs and graphenes. However, the properties of AgNW–FTCFs have been limited because of factors such as the high junction resistance and surface roughness, large

haze, big non-uniformity, and low adhesion to the surface of substrates, etc. At present, the ideal performances of AgNW–FTCFs with high conductivity and transparent are still in its infancy. Generally, it is challenging to fabricate a high-performance AgNW–FTCF with both excellent conductivity and high transmittance because AgNWs are not transparent. There are several factors affecting the optoelectronic properties of AgNW films, such as the length and dimension and purity of AgNW, the distribution of AgNWs on the substrate, the thickness of film, and the preparation method and post-treatment process of the film [5–9]. Low haze and high uniformity are two essential factors for high-end applications of the AgNW–FTCFs.

Effects have been devoted to improving the performances of AgNW–FTCFs, such as the use of long and thin AgNWs [5–7], post-treatment (heating, pressing, or illumination by a laser) [8, 9], the medium introduction [10], and coating with PEDOT: PSS [11, 12] or graphene [13] or carbon nanotube [14], etc. Araki and colleagues [15] reported that electrode composed of AgNWs with lengths up to 230 μm (mainly distributed in the range 20–100 μm) and a diameter of 91 nm showed a low R_s of 24–109 Ωsq^{-1} and a low haze of 3.4–1.6% under visible light in the T range 94–97% [15]. Wang et al. [16] prepared AgNWs electrodes with sheet resistances of 15.6 Ωsq^{-1} and 204 Ωsq^{-1} and transmittances of 90 and 97.5%,

✉ Y. H. Wang
wangzsedu@126.com

¹ Department of Materials and Food, University of Electronic Science and Technology of China Zhongshan Institute, Zhongshan 528402, China

² School of Materials and Energy, University of Electronic Science and Technology of China, Chengdu 610054, China

respectively, by washing pre-treatment process, increasing the number of washing cycles leads to the gradual reduction in the thickness of PVP layer from 13.19 to 0.96 nm. Jiu et al. [17] developed a high-intensity 15 pulsed light (HIPL) sintering technique to rapidly and simply sinter AgNW film and achieved strong adhesion and even high conductivity on these flexible polymer substrates. Sohn et al. [18] presented hybrid transparent conducting films based on AgNWs and graphene through dual co-doping method by applying various dopants (HNO_3 or Au for p-doping and N_2H_4 for n-doping) on top and bottom sides of graphene and found that the p/p-type dual-doped graphene and its hybrid formation with AgNWs appeared to be the most effective in enhancing the electrical properties of conductor (doped graphene with $\Delta R/R_0=84\%$ and AgNW/doped graphene hybrid with $\Delta R/R_0=62\%$), demonstrating doped monolayer graphene with high optical transmittance ($T=97.4\%$), and sheet resistance ($R_s=188 \Omega \text{ sq}^{-1}$). Kim et al. [10] proposed a chemical treatment using 1,8-diazabicyclo[5,4,0]undec-7-ene (DBU), to improve the conductivity of AgNWs-networked transparent conductive films by removing the surface oxide of the wires.

AgNW–FTCFs traditionally are fabricated by spray coating, spin coating, Meyer rod coating, and printing techniques. Until now, many works have also focus on control the topology of AgNWs networks and AgNWs distributions. However, very few systematic experimental study have evaluated the relationship between the electro-optical properties and microstructure of AgNW–FTCFs. In recent years, our groups have also done a lot of research works in the preparation of AgNWs with well-controlled morphologies and applications in the FTCFs and conductive adhesive [19–24]. We have been trying to understand the relationships of the morphology of AgNWs, preparation and topology and properties of AgNW–FTCFs and obtain high-performance of AgNW–FTCFs.

A key issue in preparing the high-performance of AgNW–FTCFs is the formation of the large area, uniform, thin, orderly overlapping of AgNWs conductive network. This paper presents the first detailed study for the formation of AgNWs conductive network using Meyer rod without any post-treatment. Further the electro-optical properties and microstructure characterizations of AgNW–FTCFs films were conducted to identify changes in such properties and the extent of these changes as functions of the concentration and amount of AgNWs.

2 Materials and methods

2.1 Materials

An AgNWs suspension was purchased from Suzhou Gushi New Materials Co., Ltd., China. The suspension contained

AgNWs with an average diameter and length of 25 nm and 15.5 μm , respectively, dispersed in isopropyl alcohol at a concentration of 10 mg mL^{-1} . Polyethylene terephthalate (PET) substrates were purchased from Hefei Microcrystalline Materials Co., Ltd., China. Ethanol absolute (99.7%) was purchased from Jinan Liyang Chemical Co., Ltd., China. All the chemicals were used as received.

2.2 Method

The AgNWs suspension was agitated in an ultrasonic bath before use. A controlled amount of AgNWs suspension was injected into the wedge formed between PET substrate ($50 \times 30 \text{ mm}^2$) and Meyer rod (No.7, R.D. Specialties Co., Ltd., America) and was entrapped there by capillarity. The Meyer rod was moved at the speed of 0.03 mm/s. Thus the liquid meniscus was dragged horizontally across the substrate surface. AgNWs are deposited from meniscus to substrate during the motion. Our coating process was performed at 26 °C and 50–60% relative humidity. The wet film is air dried at room temperature for 15 min.

2.3 Characterizations

The surface morphologies of the AgNW films were observed using SEM (Zeiss Sigma 500) and atomic force microscopy (AFM; Dimension Edge, Bruker, USA). The sheet resistance values of films were characterized using a four-probe system (ST2253, Suzhou Jingge Electronic Co., Ltd.) and optical transmittance values were measured using a thin-film transmittance meter (GZ502A, Shanghai Guangzhao Photoelectric Technology Co., Ltd., China). Diffuse reflectance was measured with an ultraviolet–visible spectrophotometer (760CRT, Shimadzu Ltd., Japan). Transmittance and sheet resistance of the AgNW–FTCFs were measured at twenty different sites, from which average values were calculated. T and diffuse reflectance were measured using a PET film as a reference.

3 Results and discussion

In order to understand the effects of AgNWs concentration on the formation and optoelectronic properties and microstructures of FTCFs we prepared FTCFs consisting of AgNWs with concentrations of 1.7, 2.0, 2.5, 3.3, and 5.0 mg mL^{-1} , respectively, and 0.06 mL using Meyer rod on PET substrates. Figure 1 shows schematic diagram of the fabrication of an AgNW–FTCFs using Meyer rod. Figure 2a and b present the transmittances and sheet resistances of AgNW–FTCFs. The inset in Fig. 2a contains photographs of samples. As Meyer rod moves, the deposition of AgNWs is formed in the meniscus through a convective

flux generated by the evaporation of solvent and by the lateral capillary forces. To the formation of a continuous uniform AgNWs network onto a substrate, there needs to be appropriate conditions among the Meyer rod speed, the rate and amount of AgNWs deposition, and the distribution of AgNWs in the meniscus. Obviously, the distribution of AgNWs in the meniscus and the rate of AgNWs deposition and the Meyer rod speed at our experimental conditions are constant, the deposition amount of AgNWs is proportional to the AgNWs concentration. The more the AgNWs deposition, the more the formation of the effective conductive network, and the more uniform of the resistance distribution of AgNW–FTCF. However, this does not mean that the better the optoelectronic properties of the AgNW–FTCF. When the AgNWs concentrations are 1.7, 2.0, 2.5, 3.3, and 5.0 mg mL⁻¹, respectively, the transmittance of the films at 550 nm are 94%, 92%, 90%, 89%, and 84%, respectively, and the sheet resistance of the films are 502, 244, 127, 38, and 12 Ω sq⁻¹, respectively. It is clearly that the increasing of the of AgNWs concentration led to the deposition density of film increased, which results in decreasing of the transmittance of film. However, the tighter contact among the randomly

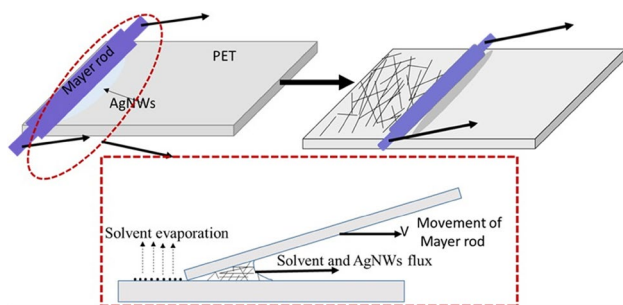


Fig. 1 Schematic diagram for fabrication of AgNW-FTCF by Meyer rod

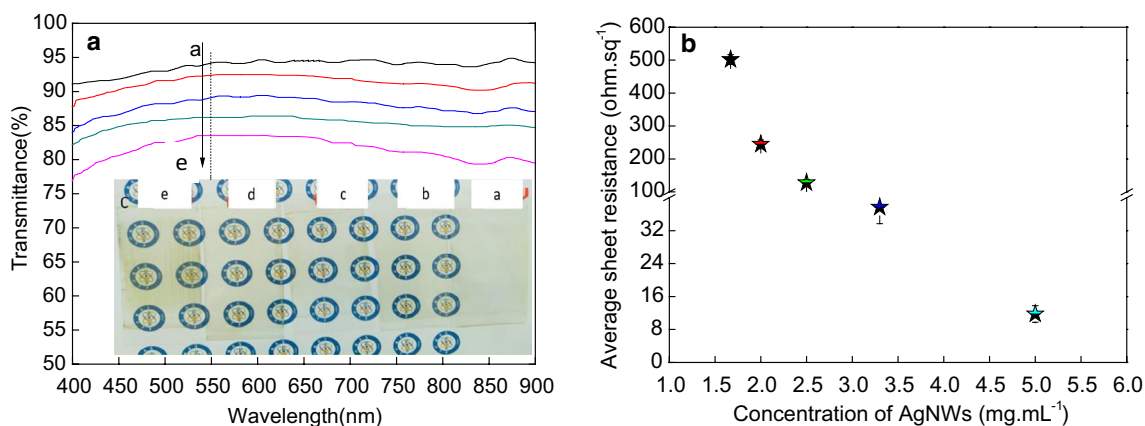


Fig. 2 **a** Transmittance and **b** sheet resistance (**b**) of films with different AgNWs concentrations. The insert in Fig. 2a contains photos of samples. Curves and photos from a to e in (**a**) are samples with AgNWs concentrations of 1.7, 2.0, 2.5, 3.3, and 5.0 mg mL⁻¹, respectively

AgNWs networks enhanced conductivity. As the transmittance of film at 550 nm increased from 90 to 92%, the sheet resistance of the film maintained in the range of 127–502 Ω sq⁻¹, indicating the thin AgNW caused the high junction resistance due to the small contact area. Obviously, the influence of the deposition density of AgNWs on the conductivity of film is much greater than that on the optical transparency of film, indicating that the appropriate concentration is beneficial to obtain the high-performance AgNW–FTCF.

SEM analysis provided an explanation for the influence of the deposition density of AgNWs on the optical and electric performances of the AgNWs films. Figure 3a–e show a series of SEM images taken on the films with AgNWs concentrations of 1.7, 2.0, 2.5, 3.3, and 5.0 mg mL⁻¹, respectively. Figure 3 reveals that with increasing of AgNWs concentration, the deposition density of AgNWs on the substrate surface increased, and the randomly distributed AgNWs overlap and stack to form a network structure.

Jia et al. defined a non-uniformity factor (*NUF*) to evaluate the standard deviation of the sheet resistance of films from the average value as follows [25],

$$NUF = \sqrt{\frac{\sum_{i=1}^n (R_i - \bar{R})^2}{n\bar{R}^2}} \quad (1)$$

where *n* is the number of measurements of the film of different sites, and *R_i* and \bar{R} are the measured resistance and average resistance for all the measurements, respectively. The smaller *NUF*, the more uniform the film. According to this method, we divided film into 24 regions of the same size, measured the sheet resistance of each region and recorded the data.

Figure 4 presents *NUF* of the sheet resistance of films consisting of AgNWs of different concentrations. The inset in Fig. 4 is the test photos of the same sample in different

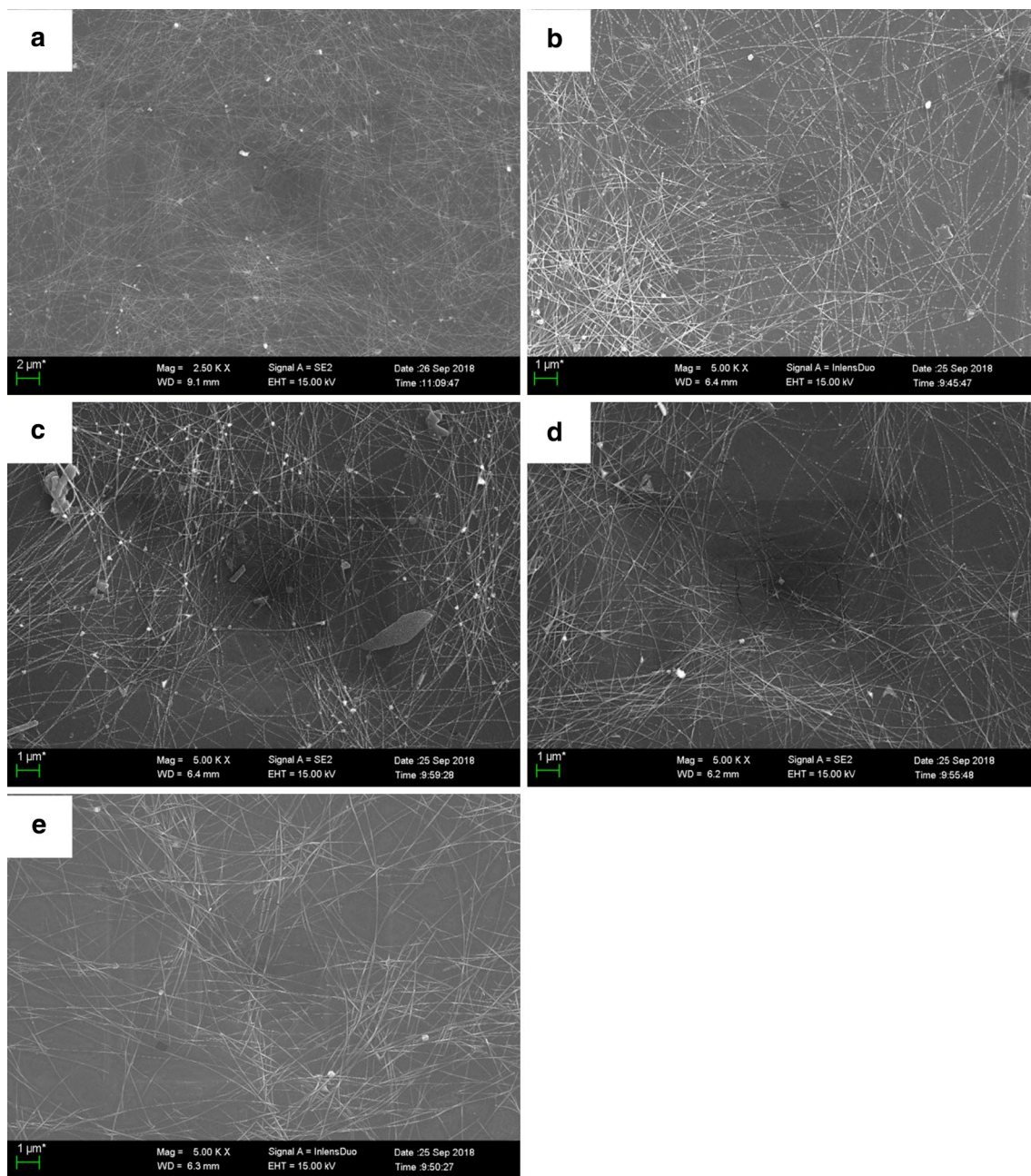


Fig. 3 SEM images of films with AgNW concentrations of **a** 1.7, **b** 2.0, **c** 2.5, **d** 3.3, and **e** 5.0 mg mL⁻¹

sites. With increasing of the AgNWs concentration, *NUF* decreased, indicating that the uniformity of sheet resistance of AgNW–FTCFs increased, which means the uniformity of distribution of AgNWs on substrate surface increased. This can be illustrated by depositing of AgNWs on the substrate surface during the process of Meyer rod, as shown in Fig. 1. For the formation of a uniform and continuous conductive AgNWs network on a substrate, the speed of movement of Meyer rod should be equal to the rate of AgNWs distribution formation [26]. The

higher AgNWs concentration, more AgNWs deposition on the substrate surface. Our experiments indicate that 1.7–2.0 mg mL⁻¹ AgNW is slightly low in this case, the continuous conductive networks are not formed well. In addition, the *NUF* values in our experiment are significantly smaller than those reported in the literature [25, 27]. It is possible to be related to the AgNWs morphology and conditions of process.

To further study the effect of AgNW concentration on the film topography, the films with AgNW concentrations

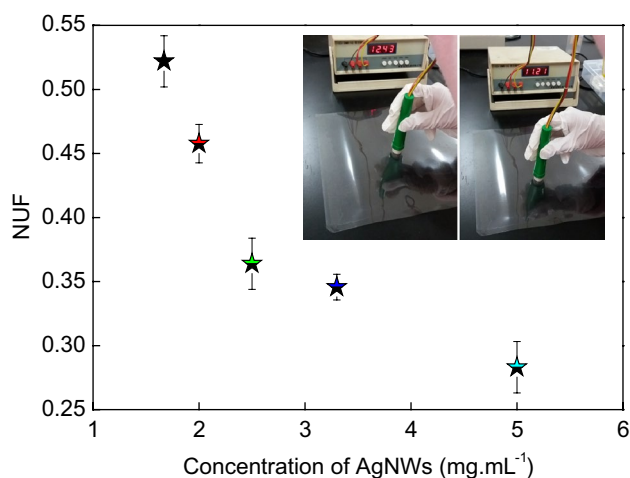


Fig. 4 Comparison of the *NUF* of the sheet resistance of films versus against AgNW concentration. The inset contains test photos of the same sample in different sites

of 1.7, 3.3, and 5 mg mL⁻¹ were analyzed by AFM as shown in Fig. 5.

The measured root mean square roughness (*RMS*) values of the film with AgNWs concentrations of 1.7, 3.3, and 5 mg mL⁻¹ were 10.9 nm, 11.3 nm, and 18.6 nm, respectively. These *RMS* values are low approximately the diameter of a nanowire. The *RMS* values of the films increases with increasing of AgNWs concentration, which may be related to the increase of the deposition density of AgNWs.

Optical haze of FTCF is one of the important factors in optoelectronic devices. Haze is defined as the ratio of diffuse transmittance to total transmittance according to ISO 14782 [28]. It is determined by the diameter and the uniformity of distribution of AgNWs on a substrate surface because the wires cause strong light scattering in the visible range. Decrease of the wire diameter has been proposed as a way to weaken light scattering [29], although there have seldom

been any studies focusing on the haze because of the difficulty involved in controlling the wire diameter.

Figure 6a and b show the relationships between the optical haze of film and the AgNW concentration of and the transmittance of film at 550 nm. With increasing of AgNW concentration and transmittance of film, the haze gradually increase and decreases, respectively. When the AgNW concentrations are 1.7, 3.3, and 5.0 mg mL⁻¹, respectively, the haze value of films are 0.78%, 1.0%, and 1.1%, respectively. All of the haze values of film are close to 1%, which is lower than the typical levels of ITO of 1–3% haze [30] and that reported in the literature [15, 30]. This was attributed to the thin AgNW used in our experiments and the low roughness which can scatter less light. Low haze leads to less obscuration of transparent materials, which is highly desirable in display-based applications. When the AgNW concentration is 3.0 mg mL⁻¹, film shows the haze of 1.0% and the sheet resistance of 38 Ω sq⁻¹ and *NUF* of 0.34 at transmittance at 550 nm of 89% with only coating at room temperature

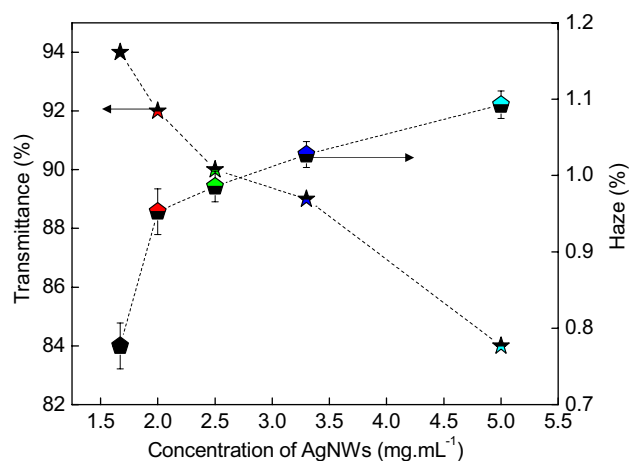


Fig. 6 Optical haze of film against **a** the concentration of AgNWs and **b** transmittance of film at 550 nm

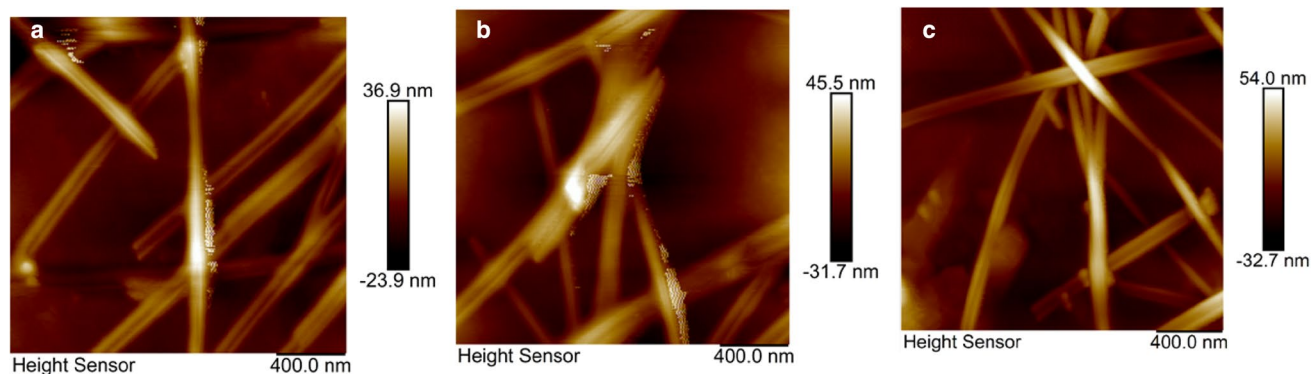


Fig. 5 AFM photographs of films with AgNW concentrations of **a** 1.7, **b** 3.3 and **c** 5 mg mL⁻¹

without any post-treatment, which are similar to the values shown by ITO film [31–33]. The above results prove that in proper conditions, we achieved the improvement in performance of the AgNW-FTCFs without any annealing steps.

Due to the film composed of AgNWs networks, the optoelectronic properties of film are defined mainly by the network morphologies which depends on the size, aspect ratio and distribution of AgNWs. Under our experimental conditions, the concentration and amount of AgNWs at the same concentration are the key factors to determine the distribution of AgNWs and deposition density on the substrate. Once the effect of the AgNWs concentration on the optoelectronic properties of film is understood, it is necessary to study the effect of the amount of AgNWs on the optoelectronic properties. Films with different AgNWs deposition densities were prepared on PET substrate using Meyer rod and with AgNWs suspension (1.7 mg mL^{-1}) amounts of 0.06, 0.08, 0.10, 0.12, and 0.14 mL, respectively. AgNW suspension (1.7 mg mL^{-1}) amounts of Fig. 7a and b show transmittance and sheet resistance and *NUF* of the sheet resistance of films consisting of AgNWs of different amounts. The inset in Fig. 7a is photographs of samples. The transmittance and the sheet resistance and the *NUF* of sheet resistance of films decreased with increasing of the amount of AgNW suspension. The film displayed the high transmittance at 500 nm of 90–95% and the low *NUF* of sheet resistance of 0.7–0.2% at the sheet resistances of 502–38 $\Omega \text{ sq}^{-1}$.

Figure 8a–d present SEM images of films consisting of AgNW suspension of 0.08, 0.10, 0.12, and 0.14 mL, respectively. Figure 8 reveals that with increasing of AgNW suspension amount, the AgNWs network become compact with a lot overlap and formed more effective interlacing percolations. In addition, agglomerations of AgNWs were observed, which indicated AgNWs have good dispersion in

suspension. The films with AgNWs suspension amount of 0.08, 0.10, and 0.14 mL were analyzed by AFM as shown in Fig. 9. The measured root mean square roughness (*RMS*) values are 11.0 nm, 12.2 nm, and 13.1 nm, respectively. These *RMS* values are low approximately the diameter of an AgNWs.

Figure 10 shows the relationships between the haze of the film and the average AgNWs amount and film transmittance at 550 nm, respectively. With increasing AgNWs suspension amount and transmittance of film, the haze value gradually increased and decreased, respectively. It is same as the effect of AgNWs concentration. The haze value is in the range 0.77–1.0% and the transmittance at 550 nm maintained 95–90% with increasing in AgNWs suspension amount from 0.06 to 0.14 mL. It is worth noting that the film consisting of the AgNWs suspension amount of 0.14 mL exhibited haze of 1.0%, sheet resistance of 38 $\Omega \text{ sq}^{-1}$, *NUF* of the sheet resistance of 0.22 at transmittance of 90% without post-treatment, which close to the film prepared with 0.06 mL of 2.5 mg mL^{-1} AgNWs except that the *NUF* value is smaller than that, indicating that the AgNWs suspension with low concentration and high amount is beneficial to obtain high performance conductive film prepared by Meyer rod method.

The films were dried in the ambient environment, so we measured the sheet resistance under the different drying time, as shown in Fig. 11. AgNW film was fabricated on PET substrates using a Meyer bar with 0.1 mL AgNWs suspension (2.5 mg mL^{-1}) and then dried in the ambient environment. When the drying time is less than 15 h, the sheet resistance of the film gradually decreased with increasing of drying time. The sheet resistances of film are about 143.9 $\Omega \text{ sq}^{-1}$ and 99.1 $\Omega \text{ sq}^{-1}$ after drying 5 min and 15 min. This was attributed to the solvent evaporation and the close connection between the AgNWs increase. After 15 h, the sheet

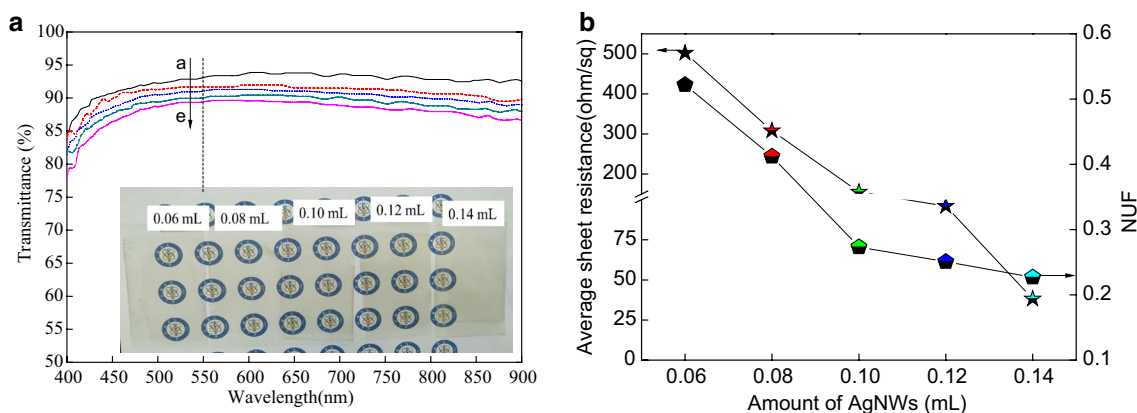


Fig. 7 **a** Transmittance and **b** sheet resistance and *NUF* of the sheet resistance of films against different amounts of AgNW suspension. The inset in Fig. 7a contains photos of samples

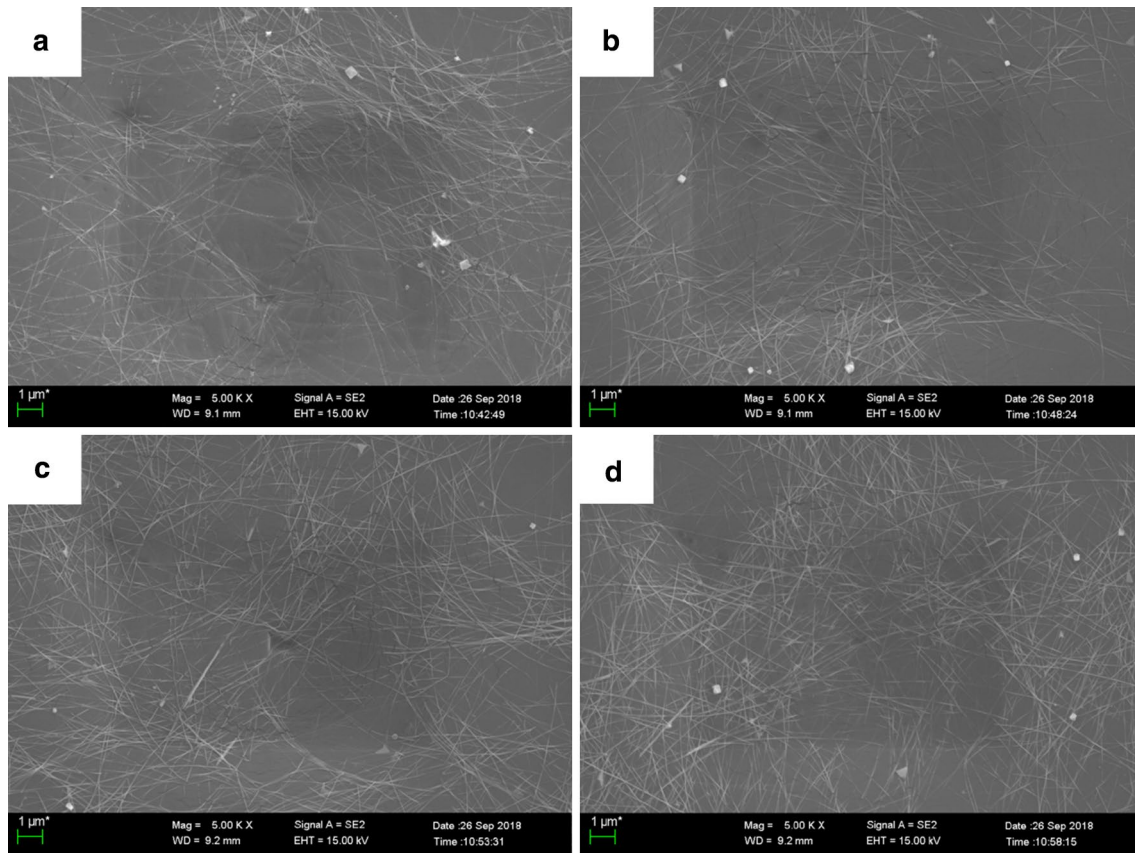


Fig. 8 SEM images of films with amounts of AgNWs suspension of **a** 0.08, **b** 0.10, **c** 0.12, and **d** 0.14 mL

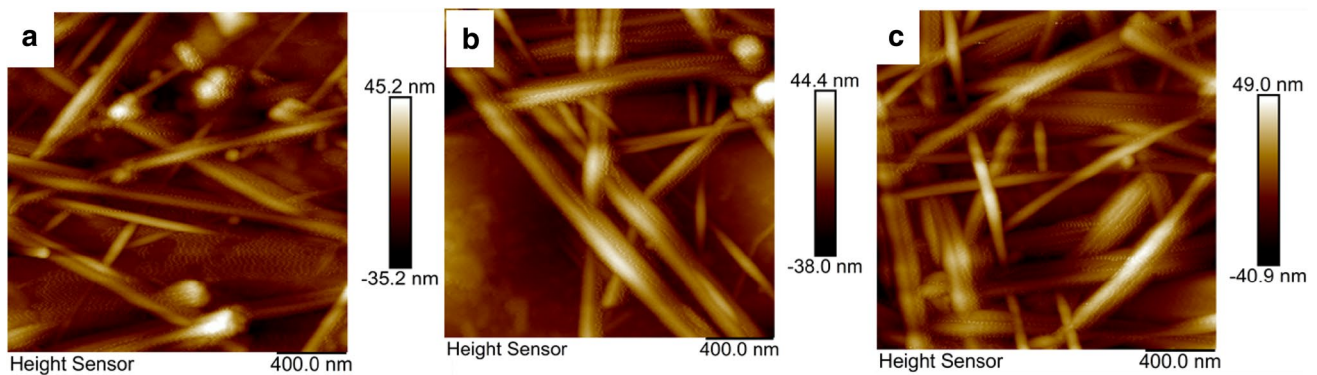


Fig. 9 AFM photographs of films with AgNW amounts of **a** 0.08, **b** 0.10, and **c** 0.14 mL

resistance of film increased slightly due to the oxidation of AgNWs. After that, the sheet resistance of film was stable.

The AgNWs conductive films are promising because of their outstanding bending properties. To illustrate the flexibility and mechanical robustness of the AgNWs film, the AgNW–FTCFs coated on the surface of cylinders with different diameters to test sheet resistance of film and the

bending tests were performed in which the films were repeatedly bent inwards or outwards. The relationship between sheet resistance of film and diameter of cylinder was shown in Fig. 12a. The film was bent inwards or outwards after 1000 bending cycles, and the sheet resistance of film with the bending cycles was shown in Fig. 12b. The inset in Fig. 12 was the testing samples. With decreasing of the

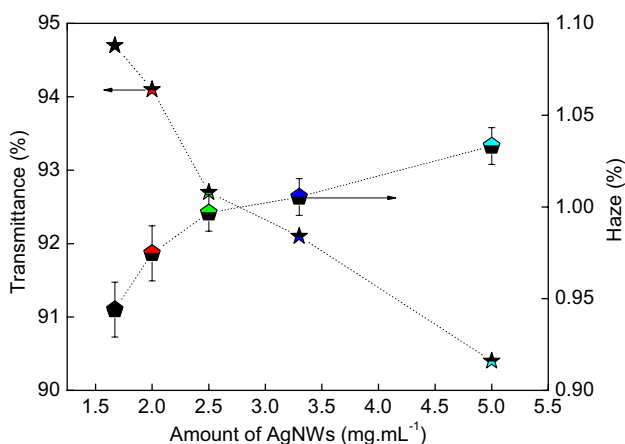


Fig. 10 Optical haze of film against **a** the amount of AgNWs suspension and **b** transmittance of film at 550 nm

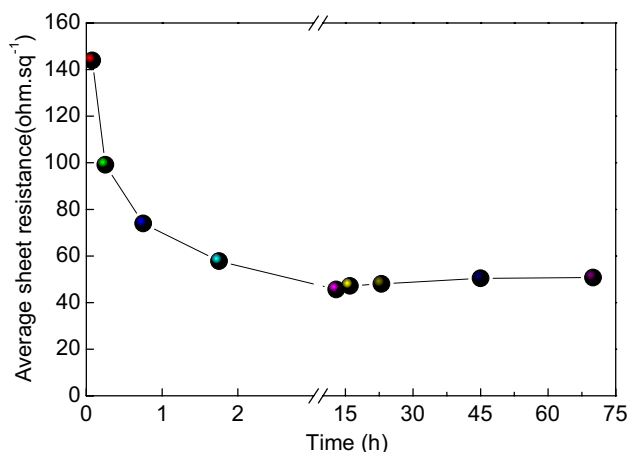


Fig. 11 Relationship of average sheet resistance of AgNW - FTCF and dry time

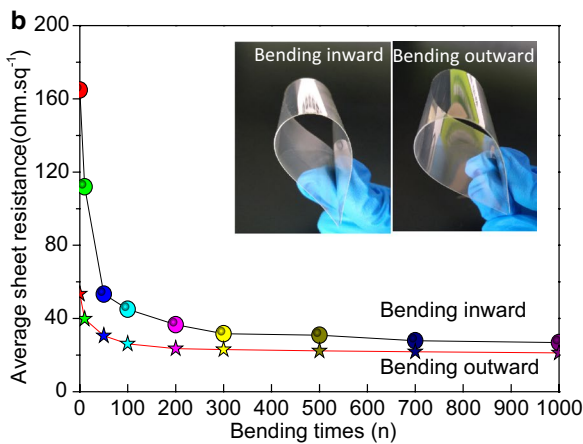
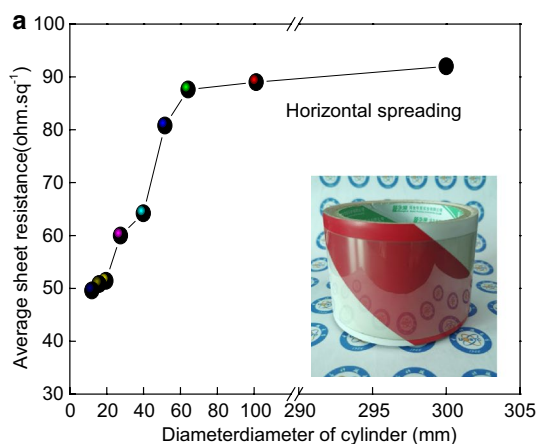


Fig. 12 Relationship between sheet resistance of AgNW - FTCF and diameter of cylinder (**a**) and bending tests (**b**)

cylinder diameter, the sheet resistance decreased, which might be that the pressure generated during bending made the nanowires contact closer and decreased the sheet resistance. However, before 200 bending cycles, the sheet resistance of AgNW film decreased with increasing of bending times. After 200 bending cycles, the sheet resistance of film tended to be stable. The highly uniform and mechanically stable AgNW transparent conductive film meet the requirement for many significant applications and could play a key role in the display market in a near future.

4 Conclusion

Transparent conductive films composed of AgNW with average diameter of 25 nm and length of 15.5 μm were fabricated by Meyer rod on polyethylene terephthalate substrates and dried in the ambient environment. We systematically investigated the effects of concentration and amount of AgNWs suspension on the optoelectronic properties and microstructures of films. The experimental results show that the sheet resistance and non-uniformity factor of the sheet resistance and the transmittance of film decrease with increasing of concentration and amount of AgNWs, while, the RMS and the haze value of the film increased with increasing of the concentration and amount of AgNWs. The AgNWs suspension with low concentration and high amount is beneficial to obtain high-performance conductive film prepared using Meyer rod. The fabricated film consisting of AgNWs suspension of 0.06–1.4 mL and 1.7–5.0 mg mL⁻¹ exhibited the sheet resistance of 12–502 Ω sq⁻¹ and the NUF of the sheet resistance of 0.2–0.7% and a haze of 0.77–1.0% at a transmittance of 84–95% and the RMS value of 10.9–18.6 nm when AgNWs.

Acknowledgements This work was financially supported by National Science Foundation of China under Grants of (61302044, 61671140) and Zhongshan Science and Technology Projects (2018SYF10).

References

1. S. Kim, B. Kim, I. Im, D. Kim, H. Lee, J. Nam, H.K. Chung, H.J. Lee, S.M. Cho, *Nanotechnology* **28**, 345201 (2017)
2. P. Wang, Z. Peng, M. Li, *Small* **14**, 1802625 (2018)
3. W.C. Chen, H.T. Lien, T.W. Cheng, C. Su, C.W. Chong, A. Ganguly, K.H. Chen, L.C. Chen, *ACS Appl. Mater. Interfaces* **7**, 4616 (2015)
4. B.P. Singh, S. Nayak, K.K. Nanda, A. Singh, C. Takai, S. Takashi, M. Fuji, *Polym. Compos.* **39**, 297 (2018)
5. Y. Zhang, J. Guo, D. Xu, Y. Sun, F. Yan, *ACS Appl. Mater. Interfaces* **9**, 25465 (2017)
6. Y. Liu, Y.Y. Chen, R. Shi, L.J. Cao, Z. Wang, T. Sun, J.J. Lin, J.Q. Liu, W. Huang, *RSC Adv.* **7**, 4891 (2017)
7. Y.X. Li, S.L. Guo, H.W. Yang, Y.X. Chao, S.Z. Jiang, C. Wang, *RSC Adv.* **8**, 8057 (2018)
8. T.C. Hauger, S.M. Al-Rafia, J.M. Buriak, *ACS Appl. Mater. Interfaces* **5**, 12663 (2013)
9. T. Tokuno, M. Nogi, M. Karakawa, J. Jiu, T.T. Nge, Y. Aso, K. Suganuma, *Nano Res.* **4**, 1215 (2011)
10. S. Kim, H.R. Jeon, C.H. An, B.-S. An, C.-W. Yang, H.-W. Lee, M. Byung, *Mater. Lett.* **193**, 63 (2017)
11. J.H. Seo, I. Hwang, H.D. Um, S. Lee, K. Lee, J. Park, H. Shin, T.-H. Kwon, S.J. Kang, K. Seo, *Adv. Mater.* **29**, 1701479 (2017)
12. J.-H. Lee, H.-S. Shin, Y.-J. Noh, S.-I. Na, H.-K. Kim, *Sol. Energy Mater. Sol. Cells* **114**, 15 (2013)
13. J. Miao, S. Chen, H. Liu, X. Zhang, *Chem. Eng. J.* **345**, 260 (2018)
14. M.X. Jing, C. Han, M. Li, X.Q. Shen, *Nanoscale Res. Lett.* **9**, 588 (2014)
15. T. Araki, J. Jiu, M. Nogi, H. Koga, S. Nagao, T. Sugahara, K. Suganuma, *Nano Res.* **7**, 236 (2014)
16. J. Wang, J. Jiu, T. Araki, M. Nogi, T. Sugahara, S. Nagao, H. Koga, P. He, K. Suganuma, *Nano-Micro Lett.* **7**, 51 (2015)
17. J. Jin, T. Sugahara, M. Nogi, T. Araki, K. Suganuma, H. Uchida, K. Shinozaki, *Nanoscale* **5**, 11820 (2013)
18. H. Sohn, Y.S. Woo, W. Shin, D.J. Yun, T. Lee, F.S. Kim, J. Hwang, *Appl. Surf. Sci.* **42**, 63 (2017)
19. X. Yang, D. Du, Y. Wang, *J. Mater. Sci.* **1**, 1 (2019)
20. D. Du, X. Yang, Y. Yang, Y. Zhao, Y. Wang, *Micromachines* **10**, 42 (2019)
21. Y.H. Wang, A. Huang, H. Xie, J.Z. Liu, Y.Z. Zhao, J.Z. Li, J. Mater. Sci. **28**, 10 (2017)
22. Y.H. Wang, N.N. Xiong, H. Xie, Y.Z. Zhao, Jingze Li, *J. Mater. Sci.: Mater. Electron.* **26**, 621 (2015)
23. Y.H. Wang, Z.L. Li, A. Hao, H. Xie, J.Z. Li, *J. Nanosci. Nanotech.* **17**, 5617 (2017)
24. Y.H. Wang, N.N. Xiong, Z.L. Li, H. Xie, J.Z. Liu, J. Dong, J. Li, *J. Mater. Sci.* **26**, 6532 (2015)
25. Y. Jia, C. Chen, D. Jia, S. Li, S. Ji, C. Ye, *ACS Appl. Mater. Interfaces* **8**, 9865 (2016)
26. A.S. Dimitrov, K. Nagayama, *Chem. Phys. Lett.* **243**, 462 (1995)
27. C. Chen, Y. Zhao, W. Wei, J. Tao, G. Lei, D. Jia, M. Wan, S. Li, S. Ji, C. Ye, *J. Mater. Chem. C* **5**, 2240 (2017)
28. G. Khanarian, J. Joo, X.Q. Liu, P. Eastman, D. Werner, K. Connell, P. Trefonas, *J. Appl. Phys.* **114**, 024302 (2013)
29. M.M. Menamparambath, A.C. Muhammed, K.H. Kim, D. Yang, J. Roh, H.C. Park, C. Kwak, J.-Y. Choi, S. Baik, *Sci. Rep.* **5**, 16371 (2015)
30. C. Preston, Y. Xu, X. Han, J.N. Munday, L. Hu, *Nano Res.* **6**, 461 (2013)
31. J.M. Gaskell, D.W. Sheel, *Thin Solid Films* **520**, 4110 (2012)
32. L. Hu, H. Kim, J. Lee, P. Peumans, Y. Cui, *ACS Nano* **4**, 2955 (2010)
33. T. Kim, A. Canlier, G. Kim, J. Choi, M. Park, S. Han, *ACS Appl. Mater. Inter.* **5**, 788 (2013)

Publisher's Note Springer Nature remains neutral with regard to jurisdictional claims in published maps and institutional affiliations.